7 Asymmetric binding of the quinone cofactor in Photosystem I as probed using ^{13}C labeled quinones

PS I complexes containing different artificial quinones that mimic certain structural parts of the native phylloquinone have been described in the previous chapter. One of the simplest cases is 2-methyl-1,4-naphthoquinone. This molecule differs from the native phylloquinone only by the absence of the phytyl side chain. In Chapter 6 the properties of 2-methyl-1,4-naphthoquinone incorporated into the A_1 site after organic solvent extraction of the native phylloquinone [78] were reported. It was found that 2-methyl-1,4-naphthoquinone can be reconstituted into the A_1 binding site with the same position and orientation as the native phylloquinone, as demonstrated by the polarization pattern and the ^1H hfs of the methyl group obtained from X- and Q-band transient EPR spectra.

To probe the electron spin density distribution over the quinone molecule in more detail, 2-methyl-1,4-naphthoquinones with ^{13}C labels in the different ring positions are used here for substitution studies. According to the X-ray structure of PS I, phylloquinone contains one hydrogen bond to the C(4)=O group. The ^{13}C label was introduced into the C4 position because this carbonyl group is involved in H-bonding and for this ring position the maximum spin density is predicted. The other ^{13}C label was introduced into the carbon position of the methyl group in order to study the spin-density distribution on the methyl group.

7.1 Efficiency of quinone replacement

For the preparation of PS I complexes with artificial quinones in the A_1 site, three different strategies have been introduced and tested to yield equivalent results [45, 78] concerning TR-EPR spectroscopy of the functional charge-separated state $P_{700}^+Q^-$:

(1) reconstitution of the quinone in PS I complexes after extraction of the native phylloquinone with organic solvent; (2) use of mutant cells in which the phylloquinone biosynthetic pathway has been interrupted (e.g. *menB* [41, 42]) and plastoquinone (PQ-9) has been recruited into the A_1 site of PS I; the artificial quinone is supplemented either *in vivo* to the growth-media or (3) *in vitro* by direct exchange of PQ-9 in PS I complexes isolated from the *menB* mutant. For the incorporation of ^{13}C labeled quinones procedure (3) was used; PQ-9 recruited into the A_1 site of PS I trimers isolated from *menB* mutant cells was replaced with differently spin labeled 2-methyl-1,4-naphthoquinones (see Figure 5.1). Substitution was considered complete when the TR-EPR spectral pattern could be considered to be pure within experimental accuracy. The lower affinity of PQ-9 in *menB* mutants than that of phylloquinone in the wild type result in a more efficient and complete incorporation of the artificial quinone.

2-methyl-1,4-naphthoquinone has been shown to enter the A_1 site in the same position and orientation as phylloquinone in wild-type PS I complexes [45, 78]. The same result is expected and confirmed here for different isotopically labeled 2-methyl-1,4-naphthoquinones.

7.2 TR-EPR investigation of PS I contained ^{13}C labeled 2-methyl-1,4-naphthoquinones

Figure 7.1 presents the X-band (top) and Q-band (bottom) spin polarized spectra of the transient radical pair state $P_{700}^{+}Q^{-}$ for the series of PS I samples with the following naphthoquinones in the A_1 site: native phylloquinone, 2-methyl-1,4-naphthoquinone, 2-methyl-4-^{13}C-1,4-naphthoquinone, 2-^{13}C-methyl-1,4-naphthoquinone. Except for the different (partially resolved) hyperfine splittings, all the transient spectra exhibit the same overall polarization pattern as native PS I, *i.e.* E/A/E (E=emission, A=absorption) at

X-band and E/A/A/E/A at Q-band. In conjunction with the well understood (high field/high frequency) spectra in wild type PS I [66, 68], this is a confirmation that the artificial quinones take up the same position and orientation as native phylloquinone in wild type. However, the polarisation patterns in Figure 7.1 differ significantly with respect to the partially resolved hyperfine multiplets. For native PS I and 2-methyl-1,4-naphthoquinone (Figure 7.1 A, B) the hfs have been described already in detail in Chapter 6, section 6.3

In Figure 7.1 (D) the same methyl hyperfine splitting is broadened beyond resolution for 2-^{13}C-methyl-1,4- naphthoquinone both at X- and Q-band, due to the additional hfs of the ^{13}C nuclear spin in the methyl group. An unchanged methyl proton hyperfine tensor was confirmed by pulsed ENDOR spectroscopy for 2-^{13}C-methyl-1,4- naphthoquinone, 2-methyl-4-^{13}C-1,4- naphthoquinone, 2-methyl-1,4-naphthoquinone and native phylloquinone (data not shown).

The X-band spectrum of the $P_{700}^{+}Q^{-}$ radical pair state with 2-methyl-4-^{13}C-1,4-naphthoquinone in the A_1 site shows the most significant differences. Correlated changes can be seen in the Q-band spectra of Figure 7.1 (C): (1) The overall spectral width is clearly larger. (2) The partially resolved hyperfine pattern becomes more complex due to the additional ^{13}C hyperfine splitting. (3) A direct indicator of a very large (out-of-plane) z-component of the ^{13}C hyperfine tensor is the additional emissive spectral component at the high field end of the both X- and Q-band spectra.

This component is specific to the spin polarisation pattern of this sample only. Corresponding spectral effects have been observed in cw Q-band spectra of bRC reconstituted with the isotope labeled ubiquinones [79, 80] and assigned to the hyperfine tensor elements of the ^{13}C spin label in the carbonyl group to which the dominant H-bond

is attached. However, even a qualitative comparison indicates that the ^{13}C hyperfine tensor elements are substantially larger for the quinone in PS I compared to bRC.

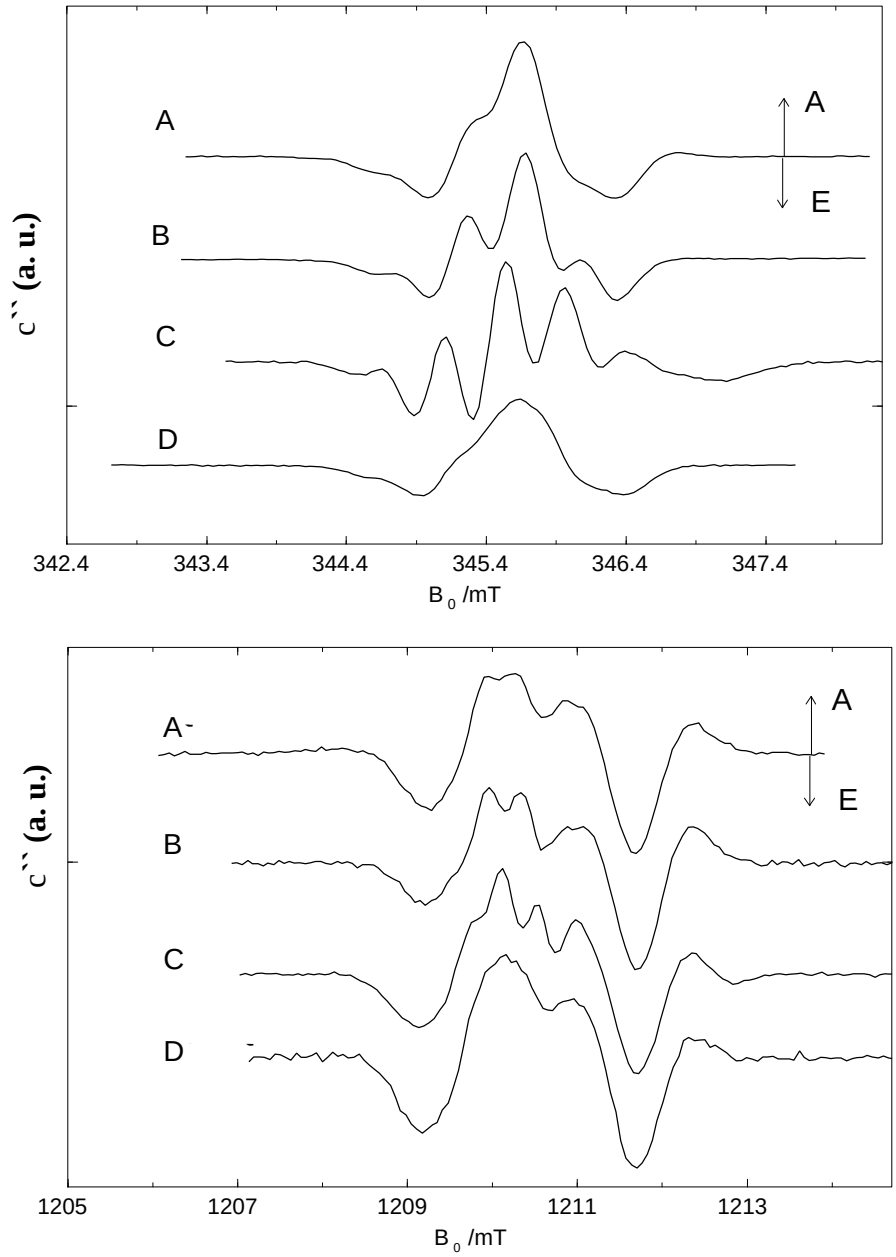

Figure 7.1 Spin polarized transient EPR spectra of the $P_{700}^{+}Q^{-}$ radical pair state in PS I particles at 80 K. Comparison of spectra with native phylloquinone (A), 2-methyl-1,4-naphthoquinone (B), 2-methyl-4-^{13}C-1,4-naphthoquinone (C), 2-^{13}C-methyl-1,4-naphthoquinone (D) in the A_1 binding site of the *menB* mutant. Top: X-band. Bottom: Q-band.

7.3 ^{13}C hyperfine tensor parameters from spectral simulations

In order to achieve a more quantitative evaluation of the ^{13}C hfs tensor elements, simulations of the transient spectra were carried out. The correlated radical pair (CRP) concept is well established and has been tested extensively [81]. A large number of magnetic interaction and structural parameters are needed for spectral simulation. Most are known from independent experimental data. Convincing spectral simulations have been achieved for the $P_{700}^{+}A_1^{-}$ state of wild type PS I [66]. Essential magnetic interaction parameters are listed in Table 6.1 with a slight adjustment of the quinone g-tensor parameters. The same relative orientation of the g-tensors of quinone and P_{700} for PS I containing 2-methyl-1,4-naphthoquinone and native phylloquinone in the A_1 site have been mentioned already. This was tested most reliably for fully-deuterated 2-methyl-1,4-naphthoquinone (Figure 6.6). The partially resolved largest hyperfine splittings due to the hfs tensors of the methyl protons and the ^{13}C spin have been considered explicitly in the simulation. However, we assume that the tensors and correlated local electronic structures remain unchanged for all isotopically labeled 2-methyl-1,4-naphthoquinones. In conclusion, for the simulation all parameters stay fixed with the exception of only two parameters of the nearly axially symmetric ^{13}C-hfs tensor.

The principal axis orientations of the ^{13}C-hf tensors coincide with those of the quinone molecular plane as known from the literature. The z-axis is collinear with the out-of-plane axis. The largest ^{13}C hyperfine splitting is expected along this axis. It will be most clearly resolved in the EPR spectra as demonstrated before on ^{13}C labeled quinones in bRC. In Figure 7.2, X- and Q-band TR-EPR powder spectra are simulated for 2-methyl-4-^{13}C-1,4-naphthoquinone in the A_1 site. The hyperfine coupling constant $A_{zz}(^{13}C)$ was varied between 36 MHz and 48 MHz (in steps of 4 MHz).

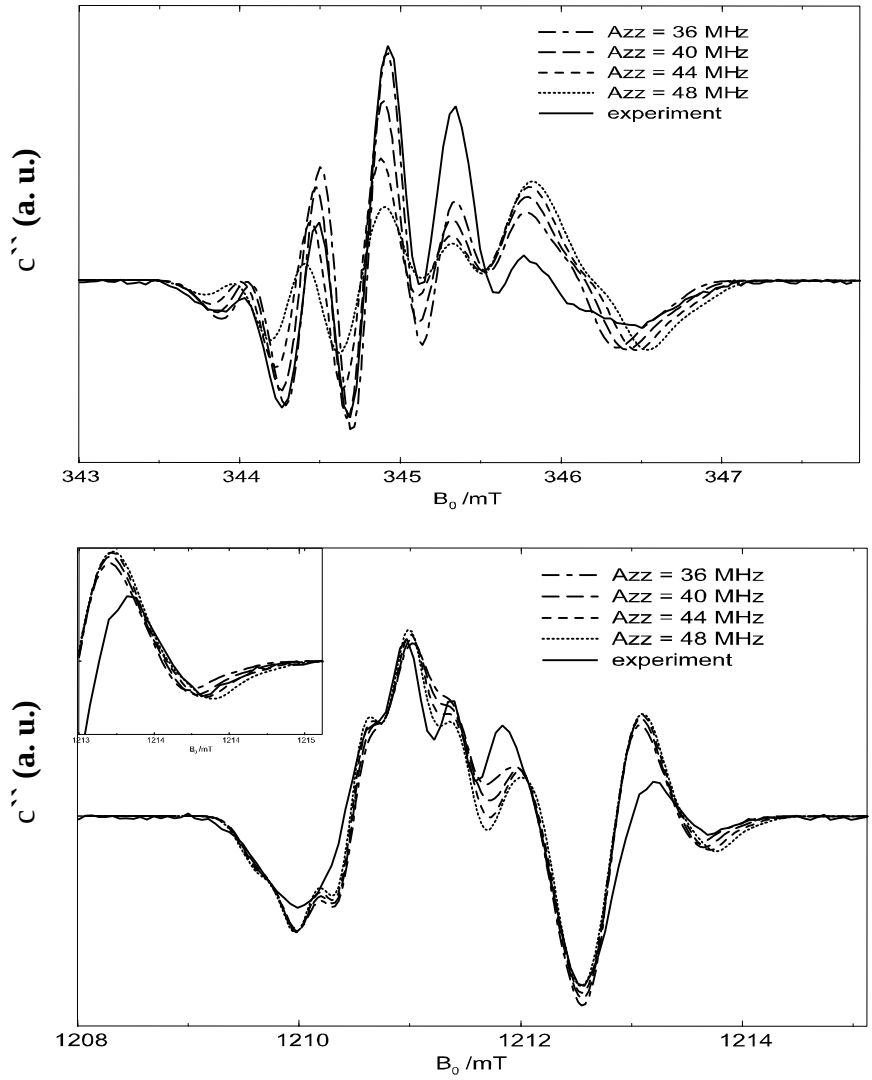

Figure 7.2 Comparison of Spin polarized transient EPR spectra of the $P_{700}^{+}Q^{-}$ radical pair state in PS I particles with 2-methyl-4-^{13}C-1,4-naphthoquinone in the A_1 binding site with simulations according to the .spin correlated radical pair model. All parameters were fixed as indicated in Tables 6.1, 7.1 and in the description of the spectral simulations. Only A_{zz} value was varied. Top: X-band. Bottom: Q-band.

Table 7.1. ^{1}H and ^{13}C hyperfine coupling (hfc) values (MHz) for different quinones in bRC and PS I

	Type I RC PhQ in PS I				Type II RC UQ in bRC		UQ_{10}^{-} in solution	PhQ in solution
	PhQ or 2-Me-1,4NQ		2-phytyl-1,4-NQ in *menG* mutant	2-Ethyl-1,4-NQ				
	$A_1^{-\cdot}$	$P_{700}^{+}A_1^{-}$						
^{1}H	$-CH_3$[a]	$-CH_3$[b]	-H[c]	$-CH_2-$[d]	$-CH_3$[e]	$-CH_3$[e]	$-CH_3$[f]	$-CH_3$[a]
$A_{x'}$ $A_{\perp}$	9.1	8.8	-15.5	12.2	3.6	3.09	4.8	6.3
$A_{y'}$ $A_{\perp}$	9.1	8.8	-11.8	12.2	3.6	3.59	4.8	6.3
$A_{z'}$ $A_{\|\|}$	12.8	12.3	$<\|-5\|$	16.8	6.8	6.62	8.5	9.5
a_{iso}	10.3	10.0	$\approx$-10.3	13.7	4.6	4.45	6.0	7.4
^{13}C								
$*A_{zz} = A_{\|\|}$	44				35.5			
$A_{xx}=A_{yy}$ $=A_{\perp}$	-9-12				$<\|-7\|$			
a_{iso}	8-9				>7			
					[g]	[j]	[i]	
$A_{zz}(^{13}C_1)$	n.d.				22.7	22.4	28.0	
$*A_{zz}(^{13}C_4)$	44				35.0	35.5	30.8	

*values for the carbon atom of the carbonyl group participating in the stronger hydrogen bond. O(2) and C(4) are atoms of the carbonyl group accepting stronger hydrogen bond
[a] Reference [40], [b] Reference [67], [c] Reference [44], [d] Reference [78], [e] Reference [38], [f]Reference [82], [g] Reference [83], [j] Reference [79], [i] Reference [84].

Most sensitive for this parameter appears to be the shift of the emissive high field component in the spectra. Best agreement with the experimental spectra is achieved for A_{zz}=44MHz. The additional hfs multiplet splitting observed in the lower field region of the X-band spectra enables an estimation of the A_{xx} and A_{yy} hfs values in the 9-12 MHz range. These ^{13}C-hfs tensor values are included in Table 7.1 which compares the combined data base for bRC and PS I.

7.4 Interplay between the asymmetric hydrogen bond and high spin density on the C(4) atom in the quinone in PS I.

This study extends the determination of the asymmetric spin density distribution to other significant ring positions of the quinone in the functional $P_{700}^{+}A_1^{-}$ state of PS I. An unusually large increase in spin density at the ring position of the methyl group of native phylloquinone in PS I has been established in many experiments [40, 67]. In addition, the increased spin density was even found to be almost independent of the substituent in this ring position. Nearly the same spin density is evaluated from the hyperfine tensor components measured for the aromatic C-H fragment in this ring position when 2-phytyl-1,4-phylloquinone occupies the A_1 site in PS I from the *men*G mutant (Table 7.1) [44]. Although it still needs to be fully explained why an n-alkyl chain goes into the position of the methyl group in native phylloquinone, the hyperfine tensor measured for the first methylene group is again consistent with quantitatively the same increased spin density in this ring position [78]. The increased a_{iso} value in this case is caused by a certain conformation of the alkyl substituent with respect to the dihedral angle θ=30° between the plane of the C-C and C-H bonds and the axis of the p_z orbital. The data collected in Table 7.1 allow the spin density shifts to be quantified. For this we can choose a comparison of the hfs constant a_{iso} of the respective CH_3 group of the quinone acceptor in the Q_A site of bRC *versus* in the A_1 site of PS I. Because the dominant H-bond is attached to opposite carbonyl groups (with respect to the same ring position for the phytyl/isoprenyl chain), the a_{iso} value of about 6.1 MHz (for ubiquinone) and 7.4 MHz (for phylloquinone) in the symmetric H-bond situation in solution are shifted in opposite directions, i.e. down to about 4.5 MHz in bRC but up to about 10 MHz in PS I (see Table 7.1). Therefore,

the absolute change is about 2 times larger in PS I. With the new results in this work we can extend this comparison to the carbon ring position of the carbonyl group which receives the dominant hydrogen bond.

Compared to the proton hfs, the theory of isotropic ^{13}C splitting is more complicated because it is not directly proportional to the π-electron spin density at the carbon atom. As a result, McConnell's relation $a_{iso} = Q*?^{p}$ no longer holds for ^{13}C splittings. Instead the splittings in aromatic radicals conform rather well to the equation: $a_{iso} = Q_1\rho_1+Q_2(\rho_2+\rho_3)$, ($Q_1$ is positive and Q_2 is negative). The largest contribution, which is proportional to the π-electron spin density ρ_1, comes from the exchange coupling between the $2p_z$ electron and the paired 1s and 2s electrons. The unpaired π-electrons on the adjacent atoms polarize the spins in the C-C σ bonds and induce negative spin densities in the C1 2s orbital which are proportional to ρ_2 and ρ_3. Many studies have been performed for ^{13}C labeled quinone anion radicals in protic and aprotic solvents such as isopropanol and dimethoxyethane. a_{iso} parameters obtained in those experiments were always quite small and never exceeded 1-2.5 MHz with somewhat higher values in the case of aprotic solvents [84, 85]. For the quinone radical in the binding site of the protein, the a_{iso} parameter is higher then for solution case (Table 7.1). Because A_{xx} and A_{yy} were not known with high precision, only a_{iso}= 7 MHz was estimated for the ubiquinone ^{13}C label in the carboxyl group accepting the stronger hydrogen bond in the bRC. In our experiment, we detected a_{iso}=9-8 MHz for the 2-methyl-4-^{13}C-1,4-naphthoquinone in PS I. The increase in a_{iso} can be readily understood if the model that correlates asymmetric H-bonding with the alternating π-spin density distribution is applied. Compared to the solution (symmetric) case, the dominant hydrogen bond with the protein will lead to an increase of spin density ρ_1 and a decrease of spin densities ρ_2 and ρ_3 on adjacent atoms, which will lead to an increase of a_{iso} because the parameter Q_1 is positive and Q_2 is negative. Although the a_{iso}

parameter also reflects the hydrogen bond influence, it can not be used for more detailed comparisons for the following reasons. First, a_{iso} is usually a small difference between two large numbers and therefore it is very sensitive to the overall spin density distribution. Second, a_{iso} can not be determined experimentally with high precision in a solid state experiment. In this situation the parameter A_{zz} of the ^{13}C hfs tensor seems to be quite practical for the purpose of comparison because it depends mainly on the unpaired electron density on the $2p_z$ orbital and can be measured reliably. The largest component A_{zz} of the ^{13}C hyperfine tensor is shifted up to 35 MHz in bRC but to 44 MHz in PS I compared to an average value of about 29 MHz for the symmetric H-bond situation in solution. Again the relative change is a factor of about 3 larger in PS I *versus* bRC. The alternating and more asymmetric spin density distribution is therefore quantitatively confirmed for another significant ring position of the quinone in the A_1 site of PS I. The applicability of the simple valence bond model (see Figure 7.3) with similarly increased spin densities in this ring position is demonstrated as well.

An additional control of the reliability of this kind of analysis can be done if the ^{1}H a_{iso} and ^{13}C A_{zz} parameters obtained for quinone in PS I are compared with the same values for the protonated quinone anion which represents the limiting case (of a maximally strong hydrogen bond) when the proton is covalently bonded to the semiquinone radical. For example, the value of ^{1}H a_{iso}=14 MHz obtained experimentally for the protonated 1,4-benzoquinone anion radical [86] for the C-H fragment in the position of high spin density. It is higher than a_{iso}=10 MHz for the same position in PS I. Another theoretical study [87], devoted to the systematic analysis of protonated, doubly protonated, hydrogen bonded and doubly hydrogen bonded 1,4-benzoquinone anion radicals results in ^{13}C $A_{zz} \approx 75$ MHz for a protonated 1,4-benzoquinone. The fact that both of our experimental values are below the limiting case, which can never be realised in PS I, additionally supports the model.

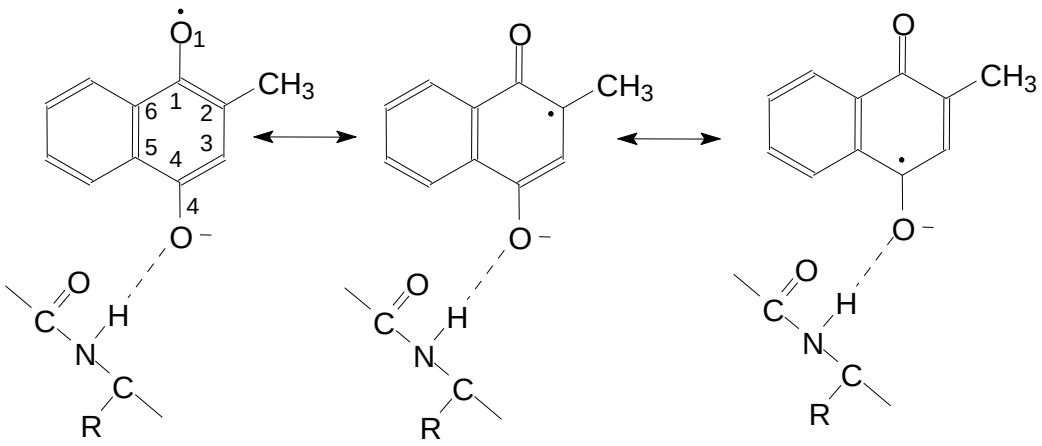

Figure 7.3 Valence bond model used to explain the spin density distribution of a 1,4-naphthoquinone anion radical hydrogen bonded to the back bone nitrogen. Note that for a hydrogen bond oxygen atom the electrostatic interaction of the partial positive charge at the proton increases the charge density at hydrogen bonded oxygen and decreases it in the ring and at oxygens without s hydrogen bond. Concomitantly, the spin density is increased at the position marked with the $^{\cdot}$ (point).

Next we can ask about the state of quantum chemical calculations of magnetic resonance parameters of quinone + protein environment models. In the case of PS I, DFT calculations have so far focused on g-tensors [88]. Hyperfine tensors have not received equal attention so far. Moreover, the protein cofactor interactions of p-stacking and H-bonding generally lead to compensating effects on both the g-tensor anisotropy and hyperfine tensor parameters. Calculations on a model system with 2-methyl-3-propenyl-1,4-naphthoquinone asymmetrically hydrogen bonded via the O4 oxygen to the nitrogen of a methyl-imidazole group resulted in a value (A_{zz}=22 MHz) [69] well below the values determined experimentally. It should be pointed out that these calculations did not take into account the π-stacking interaction between the quinone and the nearby tryptophan. This calculated value shows a surprisingly large deviation from the experimental value. In fact

the A_{zz}=26 MHz calculated for the corresponding quinone in solution (modelled by four methanol molecules) is even closer to the experimental value.

Based on the study of ^{13}C labeled quinones we conclude that the single strong hydrogen bond between the protein and quinone leads to the unusually high asymmetry in the spin density distribution. For a further discussion of the possible reasons for the strengthening of the hydrogen bond, see Chapter 11.